

PROTEIN-PROTEIN INTERACTIONS *IN VIVO*: USE OF BIOSENSORS BASED ON FRET

Jan Willem Borst^{1,2}, Isabella Nougalli-Tonaco³, Mark A. Hink^{1,2},
Arie van Hoek^{1,4}, Richard G.H. Immink⁴ and Antonie J.W.G.
Visser^{1, 2, 5}

15.1. INTRODUCTION

Sensing of molecules in living cells is a rapidly evolving discipline in modern biological and biomedical research. Biosensors make use of biological components to sense a molecule of interest. In the food, health care and pharmaceutical industry the biosensor technology is the prime developing target for the future. Optical biosensors are ideal candidates for industrial use because of the high specificity, selectivity and adaptability (Terry et al., 1995). A typical example is the application of disposable blood glucose biosensors, in which blood sugar levels of diabetic patients are monitored in real time (Wilson and Gifford, 2005). Biosensors used in cell biology generally imply real-time monitoring of molecular behavior activities or interactions of molecules in living cells (Bunt and Wouters, 2004). Many of the biosensors used nowadays are based on the Förster Resonance Energy Transfer FRET methodology. FRET is a fluorescence technique based on dipolar interactions between different donor and acceptor molecules making this technique very sensitive to intermolecular distances (Clegg, 1996; Wouters and Bastiaens, 1999; Berney and Danuser, 2003; Jares-Erijman and Jovin, 2003; Gadella et al., 1999; Lakowicz, 1999). The main principles of FRET have been summarized in Table 15.1.

¹ MicroSpectroscopy Centre, Wageningen University, Dreijenlaan 3, 6703 HA Wageningen, The Netherlands

² Laboratory of Biochemistry, Wageningen University, Dreijenlaan 3, 6703 HA Wageningen, The Netherlands

³ Plant Research International, Bioscience, Bornsesteeg 65, 6708 PD Wageningen

⁴ Laboratory for Biophysics, Wageningen University, Dreijenlaan 3, 6703 HA Wageningen, The Netherlands

⁵ Department of Structural Biology, Faculty of Earth and Life Sciences, Vrije Universiteit, 1081 HV Amsterdam, The Netherlands

Table 15.1: FRET Theory

<ul style="list-style-type: none"> The fluorescence lifetime provides a time window for the detection of dynamic processes Dynamic processes that compete with fluorescence: <ul style="list-style-type: none"> quenching by external molecules resonance energy transfer (rate constant k_T) The fluorescence lifetime of the donor becomes shorter in case of RET. 	
<p>Donor</p> <p>$\tau_D = \frac{1}{k_r + k_{nr}}$ Becomes $\tau_{EM} = \frac{1}{k_r + k_{nr} + k_T}$</p>	<p>Summary of FRET parameters</p> <p>$R_0 = 0.211 (\kappa^2 * n^4 * Q_D * J)^{1/6}$ (in Å)</p> <p>κ^2 = dipole orientation factor ($0 < \kappa^2 < 4$) (for random and rapid orientations: $\kappa^2 = 2/3$)</p> <p>Q_D = quantum yield of the donor ($Q_{CFP} = 0.39$)</p> <p>J = spectral overlap between donor emission and acceptor absorbance spectra ($J = 1.55479 \times 10^{13} \text{ nm}^4 \text{ M}^{-1} \text{ cm}^{-1}$ (CFP-YFP))</p> <p>n = refractive index of the sample ($n = 1.4$).</p>
<p>Ex → [CFP] → Em Ex → [YFP] → Em</p> <p>$R < 1.5 R_0$ $R \gg 1.5 R_0$</p> <p>R_0 = critical transfer distance, for CFP-YFP $R_0 = 5.0 \text{ nm}$</p> <p>Absorbance, fluorescence vs Wavelength, nm</p>	<p>Efficiency vs R/R_0</p> <p>$E = \frac{R_0^6}{R_0^6 + R^6}$</p>
<p>The actual distance R is obtained from the transfer efficiency $E = R_0^6 / (R_0^6 + R^6)$</p> <p>Example in case of donor CFP and acceptor YFP $\tau_D = 2.6 \text{ ns}$ (no FRET) $\tau_{DA} = 1.3 \text{ ns}$ (FRET)</p> <p>$E = 0.5 \Rightarrow R = R_0 = 5.0 \text{ nm} \Rightarrow$ actual and critical distances are the same</p>	

New developments of optical biosensors in combination with fluorescence microscopy give insight in the responses of molecular components in the cell such as receptors, proteins or ligands, which are activated in a dynamic network. Classical biochemical approaches mostly referred to as *in vitro* experiments, have been proven to be valuable for identification and physical isolation of proteins. The cellular localization of proteins can be visualized using immunofluorescence techniques. Co-immuno-precipitation and affinity chromatography are classical biochemical techniques for purification of protein complexes. Live cell imaging provides the time as an additional dimension and has evolved as an important approach in cell biology to monitor cell dynamics (Lippincott-Schwartz et al., 2001). Nowadays localization and

dynamics can be connected with system properties like active state, mobility, electric field, oxygen, calcium or proton fluxes to address different biological questions (Wouters et al., 2001). To visualize and quantify proteins of interest, advanced spectroscopic techniques are combined with microscopy and biosensors, so that specific molecular information of cells can be retrieved (Bunt and Wouters, 2004). The application of the green fluorescent protein GFP technology has been of crucial importance in the imaging of cellular proteins (Tsien, 1998; Matz et al., 1999). GFP can be coupled to the protein of interest via genetic approaches. After transformation or transfection of eukaryotic cells its fluorescence can be detected within several hours. Since the discovery of GFP, a variety of colored fluorescent proteins was developed by mutagenesis. Fluorescent proteins emitting colors from violet to red are currently available (Verkhusha and Lukyanov, 2004; Shaner et al., 2004) and allow to monitor simultaneously multiple proteins.

The question, whether the physical state of a receptor or protein is monomeric, dimeric, or multimeric can be addressed and answered by several different approaches. The phage display method and/or yeast two-hybrid system are the most significant examples of these techniques (Burch et al., 2004; Causier and Davies, 2002). However, these methods have the disadvantage that they lack spatial information. The introduction of high-resolution confocal microscopy gave the opportunity to investigate the co-expression of different proteins in their natural environment. The optical resolution of a microscope allows detection at sub-cellular level, but physical molecular interactions between proteins or receptors on nanometer scale cannot be visualized. The resolution of a typical confocal or wide-field image is diffraction limited, which means that, for example, the use of excitation light of 488 nm will result in an optical resolution around 220 nm (Herman, 1998). One possibility to go beyond the optical limitations is to apply FRET microscopy. FRET microscopy can be monitored using different optical methods, which will be discussed in this chapter. First, the FRET combinations in cell biology and different FRET biosensors will briefly reviewed. Then, the fluorescence intensity based approaches will be discussed. Subsequently, the methodology to observe FRET with fluorescence lifetime imaging microscopy FLIM will be addressed in more detail. Plant transcription factors labeled with enhanced Cyan Fluorescent protein ECFP and enhanced Yellow Fluorescent protein EYFP in plant cells will serve as an example.

15.2. FRET COMBINATIONS IN CELL BIOLOGY

Which FRET pair is the best choice? The most attractive method to add a fluorescent label is by genetic approaches (Hink et al., 2002). Visualization of proteins of interest in plant or animal cells requires *in vivo* labeling using different fluorophore combinations. The enhanced forms of CFP and YFP are most commonly used in cell biology. The main reasons for that are the attractive spectroscopic characteristics of this FRET pair: i the spectral overlap between the donor emission and acceptor absorption is large ii the donor

fluorescence lifetime ECFP is relatively short $\tau = 2.5$ ns and iii the molar extinction coefficient of the acceptor EYFP is high. The resulting Förster radius is large $R_0 = 5$ nm see Box 1, Recently, a monomeric and improved version of ECFP mCerulean has been developed, which is 2.5 times brighter than ECFP (Rizzo et al., 2004). In combination with the improved YFP version called 'Venus' mCerulean-Venus is a promising FRET pair that can be used for imaging of protein interactions in cell biology. Another frequently used combination is GFP and the Discosoma red fluorescent protein, DsRED, or related red fluorescent protein RFP. The disadvantage of DsRED as an acceptor is the maturation time, which is four times longer than for GFP. Furthermore, DsRED can tetramerize and it has a 'green' absorption band, which overlaps with the absorption band of GFP. Since 2002 several different red fluorescent proteins, dimer and monomer versions of DsRED have been cloned (Campbell et al., 2002; Zhang et al., 2002; Shaner et al., 2004). Recently, FLIM data of GFP tagged protein in combination with monomeric RFP mRFP have been presented (Peter et al., 2005). A clear interaction between a chemokine receptor and protein kinase C in carcinoma cells was found after adding a stimulus to the cells resulting in a strong reduction of the fluorescence lifetime of the GFP tagged protein (Peter et al., 2005).

15.3. FRET SENSORS

There are many examples how FRET can be used in current biological research. For example, a new displacement hybridization method is reported using a FRET biosensor to detect double stranded nucleic acid targets with Hoechst 33258 and Oregon Green488 as donor-acceptor pair (Ho and Hall, 2004). The visible fluorescent proteins appear to be useful for the detection of different processes that employ the intrinsic properties of the fluorescent protein itself. It is known that GFP is sensitive to pH changes (Haupt et al., 1998; Kneen et al., 1998). The protonated form of GFP absorbs light at 400 nm and is hardly fluorescent upon 480-500 nm excitation, so that it can act as a pH sensor. Different other sensors based on GFP technology were developed, but will not be discussed in this review. Three FRET based sensors will be briefly described here below.

15.3.1 Cameleons (Ycam)

Fluorescent indicators for *in vivo* calcium imaging were developed (Miyawaki et al., 1997). Cameleons are genetically encoded fluorescent calcium indicators without cofactors and are targetable to specific intracellular locations (Miyawaki et al., 1999; Miyawaki et al., 1997). Calcium is a very important ion in cellular signaling, since it can act as an essential second messenger in signal transduction cascades. Ca^{2+} signals are found in the cytosol and different organelles, but these signals are often hard to measure. To overcome this problem a specific calcium sensor was developed consisting of tandem fusions of a CFP, calmodulin having four calcium binding sites, a

calmodulin binding peptide M13 and YFP (Miyawaki et al., 1997). The level of intramolecular FRET is dependent on the amount of Ca^{2+} binding to the calmodulin. Binding of Ca^{2+} makes calmodulin wrap around the M13 domain upon which an increase of the FRET signal will be observed. The dynamic range for Ca^{2+} concentrations is from 10^{-8} to 10^{-2} M. Several variants of cameleons are currently available and are continuously improved. The latest versions are pH independent and consist of the brighter EYFP variants Venus. Recently, also a biosynthetic indicator of endoplasmic reticulum in endocrine cells of mouse pancreas has been described based on the cameleon3.3er YC3.3er allowing real-time visualization of cell signaling in living tissues (Hara et al., 2004).

15.3.2 Caspase sensor

One of the cellular processes, which is involved in a variety of diseases, is apoptosis or programmed cell death (Mahajan et al., 1999). A class of cysteine proteases known as caspases is involved in the apoptosis process. After activation by apoptotic signals the caspases digest cellular proteins and induce cell death. These proteases exist in many isoforms and can recognize specific amino acid motifs in their target proteins (Morgan and Thorburn, 2001). A caspase sensor based on FRET was developed for *in vivo* visualization and quantification of caspase activity (Xu et al., 1998). Like the cameleon the caspase sensor consists of a tandem of cyan and yellow fluorescent protein coupled via a linker between 12 and 20 amino acids. There are several isoforms of the caspases, which recognize specific amino acid sequences. Xu and colleagues have demonstrated caspase 3 activity *in vivo* using this FRET sensor (Xu et al., 1998).

15.3.3 FLAME

Fluorescent biosensors like the cameleons are also applied for detecting intracellular phosphorylation states in which a conformational change will alter the energy transfer efficiency. Recently, a new FRET sensor the so-called FLAME fluorescent linked autophosphorylation monitor for EGFR, was developed by Bastiaens and colleagues. This FRET sensor monitors the *in vivo* phosphorylation state of the epidermal growth factor receptor EGFR signaling system (Offterdinger et al., 2004). EGFR initiation occurs by ligand EGF binding followed by homodimerization and rapid receptor autophosphorylation. To monitor EGFR phosphorylation the translocation and binding of phosphotyrosine-binding domain PTB labeled with enhanced yellow fluorescent protein EYFP to enhanced cyan fluorescent protein ECFP-tagged EGFR was measured. Expression of this FLAME sensor in COS7 cells demonstrated rapid and reversible changes in the EYFP/ECFP fluorescence intensity ratios, due to binding of the PTB domain to its consensus-binding site upon phosphorylation at the cell periphery. The results show that this sensor closely approaches the true dynamics of tyrosine kinase autophosphorylation and dephosphorylation (Offterdinger et al., 2004).

15.4. INTENSITY BASED FRET IMAGING

15.4.1 Confocal and wide-field FRET imaging

The combination of optical microscopy with FRET spectroscopy provides quantitative, temporal and spatial information about binding and interaction of proteins *in vivo* (Herman, 1998; Wallrabe et al., 2003). FRET can be quantified using steady state or time-resolved fluorescence techniques. In the steady-state approach the fluorescence intensities of donor and acceptor are monitored in a fluorescence microscope by using either confocal or wide-field illumination and detection. This steady-state approach relies on the observation that the fluorescence intensity of the donor is reduced and the acceptor fluorescence is enhanced when energy transfer takes place. The disadvantage of this approach is that the signals are highly dependent on the concentrations of donor and acceptor molecules. Photobleaching needs to be avoided, because it alters the effective donor and acceptor concentrations. Artefacts like bleed-through of the donor fluorescence in the acceptor detection channel and direct excitation of the acceptor also need to be taken into account. In several publications corrected FRET imaging methods have been demonstrated and optimized (Gordon et al., 1998; Xia and Liu, 2001).

15.4.2 Spectral imaging

Another approach is to couple a spectrograph to the microscope for determining emission spectra of microscopic objects. Spectral resolution of fluorescence can provide the necessary imaging contrast when the spectral profile changes due to modulation of energy transfer efficiency. Based on sensitized acceptor emission and donor fluorescence quenching, spectral images can be analyzed to quantify the donor-acceptor energy transfer process within a cell (Gadella et al., 1999; Raicu et al., 2005).

15.4.3 Acceptor photo-bleaching

Another method in which FRET can be used to examine intracellular molecular interactions between proteins is acceptor photobleaching APB. This method has been applied to several studies (Kenworthy, 2001) and are not only restricted to intensity-based microscopic applications, but also to fluorescence lifetime imaging microscopy FLIM (Wouters and Bastiaens, 1999). APB is often used as a method to prove the occurrence of FRET. APB measurements in a confocal microscope have been critically assessed by Karpova and colleagues (Karpova et al., 2003). These APB experiments make use of a confocal laser scanning microscope, because specific laser lines are not only able to selectively excite the fluorescent dyes, but can also specifically bleach the dye of interest. The fluorescence intensities of donor and acceptor are determined before and after applying a strong laser pulse that photobleaches the acceptor fluorophore irreversibly. When donor and acceptor molecules interact, the destruction of the acceptor fluorophore will result in increased

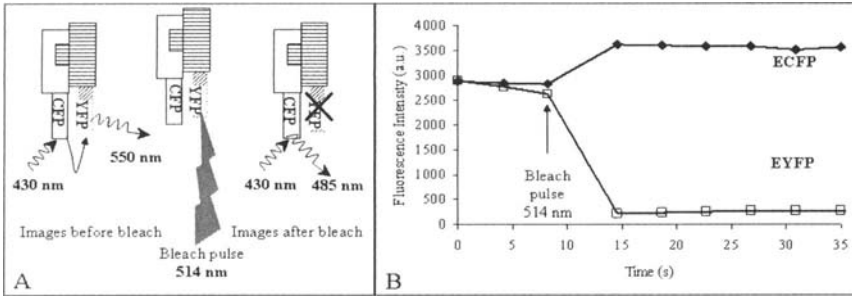


Figure 15.1. Schematic illustration of the acceptor photobleaching principle (A). Fluorescence intensity images are taken before and after a strong bleach pulse, which irreversibly destroys the acceptor molecule (YFP). The integrated fluorescence intensities of donor (CFP) and acceptor (YFP) fluorescence are measured and plotted in a graph (B).

donor fluorescence, since the energy cannot be transferred to the acceptor molecule Fig. 15.1.

The energy transfer efficiency E before the bleaching can be calculated according to:

$$E = I_{DA} - I_{DB} / I_{DA} \quad (1)$$

where I_{DB} is the fluorescence intensity before bleaching and I_{DA} is the fluorescence intensity after bleaching.

The measurement of FRET efficiency by the acceptor-photobleaching approach requires several checkpoints. First, selective bleaching of the acceptor is required, because bleaching of the donor will result in underestimation of donor dequenching (Kenworthy, 2001; Voss et al., 2005). Second, APB is still an intensity-based approach and therefore it is sensitive for donor and acceptor concentrations. By using a FRET indicator where only one CFP and one YFP molecule are connected by a linker this problem can be avoided. A general remark about the visualization and FRET determination of fluorescent proteins is that the use of strong constitutive promoters is often required. Then high expression levels of the fluorescent proteins can be reached and as a result the localization can be altered and large protein aggregates might appear. Furthermore, fluorescent proteins have the tendency to form dimers at high expression levels, although the proteins of interest are not necessarily related. It has been demonstrated that the main amino acid responsible for this “sticky” behavior of the visible fluorescent proteins is alanine 206. Replacement of this amino acid for a lysine resulted in truly monomeric fluorescent proteins (Zacharias et al., 2002). APB experiments are often performed in fixed samples. In living cells a rapid redistribution of donor and acceptor molecules may give rise to fast recovery and FRET is then difficult to determine quantitatively. APB experiments can also be combined with FLIM measurements determining the fluorescence lifetime of the donor. Interaction between a donor and an acceptor molecule will result in a faster

fluorescence decay of the donor molecule, but destruction of the acceptor molecule will reverse the quenching effect and the initial fluorescence lifetime of the donor without acceptor is obtained (Bastiaens and Squire, 1999).

15.5. FLUORESCENCE LIFETIME IMAGING MICROSCOPY (FLIM)

The fluorescence lifetime of a molecule is dependent on local environmental factors such as the presence of Ca^{2+} , effects of pH or refractive index (Suhling et al., 2002; Borst et al., 2005) or FRET. In general, the fluorescence lifetime is determined by interplay of radiative and non-radiative decay rates. The radiative decay rate is considered to be constant for a given fluorophore, while the non-radiative decay rate can vary with the environment. Most FLIM measurements for determining FRET are based on the effect that an acceptor molecule specifically interacts with a donor molecule resulting in quenching of donor fluorescence. This donor fluorescence quenching will result in the reduction of the fluorescence lifetime since energy transfer will introduce an additional relaxation path from the excited state to the ground state see Box 1. The amount of reduction is directly correlated with the FRET efficiency E via:

$$E = 1 - \tau_{DA}/\tau_D \quad (2)$$

where τ_{DA} is the fluorescence lifetime of the donor in the presence of acceptor and τ_D is the fluorescence lifetime of the donor alone.

FLIM combines fluorescence lifetime measurements with microscopic resolution resulting in spatially resolved fluorescence lifetimes. A major advantage of this approach is that the results are relatively insensitive to the local fluorophore concentration, spectral cross talk or photobleaching. Fluorescence lifetimes can be determined via time-domain or frequency-domain methods (Gratton et al., 2003; Squire and Bastiaens, 1999; Gadella et al., 1999). In short, with the frequency-domain approach the sample is illuminated with sinusoidally modulated light at frequencies typically between 20 MHz and 1 GHz. As a result the fluorescence is also sinusoidally modulated and the fluorescence lifetime is calculated from the phase shift and demodulation relative to these parameters of the excitation light (Lakowicz, 1999; Gratton et al., 2003; Squire and Bastiaens, 1999). Frequency domain FLIM measurements consist of successive recording of several images to determine spatially resolved apparent lifetimes pixel by pixel from the phase shift between excitation and emission demodulation. The time-domain method uses ultrashort excitation pulses down to hundreds of femtoseconds upon which the fluorescence decay can be measured (Hink et al., 2002; Gerritsen and De Grauw, 1999). Nowadays commercially available photon counting electronic boards are widely used and integrated with a confocal microscope system Becker et al., 2004. The board uses the time-correlated single photon counting TCSPC principle to record the arrival time of the emitted photon in

the detector with respect to the laser pulse. Another time-domain configuration is the so-called lifetime module LIMO system in which the photons are collected in four variable time windows. From the relative content of the four time gates the fluorescence lifetime can be retrieved (Gerritsen et al., 2002)

15.5.1 FLIM setup

A schematic description of the instrumental set up and how TCSPC is incorporated in the microscope set up is given in Fig. 15.2.

The here presented experiments are performed on a multi-photon dedicated Biorad Radiance 2100 MP system. The fluorescence is detected in a non-descanned manner and FLIM measurements are performed by directing the fluorescence photons via a dichroic filter 670UVDCLP onto a Hamamatsu R3809U photomultiplier tube PMT. ECFP fluorescence is selected using a 480DF30 bandpass filter. The microchannel-plate PMT allows single-photon detection at high time-resolution 50 ps. The output of the PMT is coupled to a Becker & Hickl single photon counting module SPC 830, as the start signal the single-photon timing process. The pulses from the Ti-Sapphire laser repetition rate 76 MHz serve as the SYNC or stop signal for the single-photon timing process. From the statistics of the time of arrival of fluorescence photons relative to the laser pulses the decay profile is built up. The experimental time window was divided into 64 channels and fluorescence was typically recorded for 90 seconds at a photon count rate of approximately 20 kHz. The pixel clock and line pre-divider signals from the Biorad scanhead were used to direct the single-photon timing data in appropriate memory blocks to create 2D lifetime images.

15.5.2 FLIM analysis

The FLIM data were obtained using the Becker & Hickl SPC830 acquisition card. The SPCImage 2.8 software package was used for data analysis. The software enables to fit the fluorescence decay data of every pixel in the image to a mono- or bi-exponential decay model. When in the analysis of the fluorescence data of a FRET system two decay time components are used, one fraction can directly denote the contribution of the non-interacting species donor fluorescence lifetime alone and the other fraction with a shorter lifetime component may reflect the presence of interacting molecules.

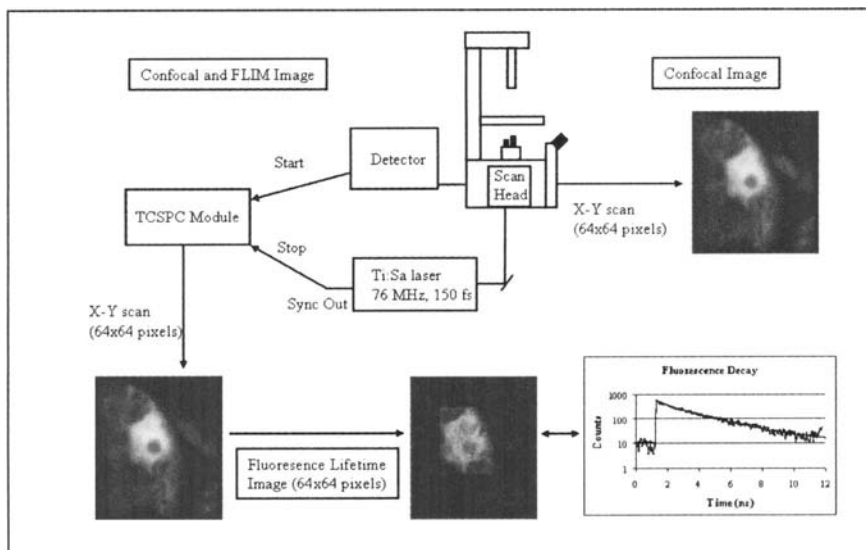


Figure 15.2. Schematic illustration of a two-photon microscope in combination with a setup for measuring fluorescence lifetimes. Besides the conventional two-photon excited confocal imaging, the microscope can also collect the photons in a counting mode, while the scanhead of the microscope is synchronized with the TCSPC acquisition card.

The analysis software has the possibility to choose a pixel binning factor. The binning occurs according to the relationship $p = (2b+1)^2$ where p is the number of pixels and b is the binning factor. All presented data were analyzed with binning $b=1$ and comparison with true 1-pixel analysis $b=0$ resulted in the same fit parameters. The image resolution was set at 64×64 pixels. The increase of the number of pixels would not enhance the resolution, because with a 60x water immersive objective lens the size of the x,y pixels reaches already the diffraction limit 250 – 400 nm.

15.6. APPLICATIONS WITH PLANT TRANSCRIPTION FACTORS

15.6.1 Sub-cellular localization via confocal microscopy

In this paragraph an application of FRET microscopy in combination with FLIM will be described. The aim is the study of MADS box transcription factor interactions in living plant cells. MADS box genes encode for transcription factors involved in many developmental process in flowering plants, most notably in the determination of floral meristem and floral organ identity (Ferrario et al., 2004; Riechmann and Meyerowitz, 1997). This family of transcription factors acts in a complex network of physical protein-protein and protein-DNA interactions either as homo- or heterodimers, and are, most likely, able to form higher order complexes (Egea-Cortines et al., 1999; Honma and

Goto, 2001). To study this network of interactions, the use of the yeast two-hybrid system has become a powerful tool to get a first impression about the ability of the MADS box proteins to form specific dimers and/or higher-order complexes. Recently, comprehensive matrix-based screens for petunia and Arabidopsis MADS box transcription factor interactions revealed the ability of these factors to form specific homo- and heterodimers (Immink et al., 2003; de Folter et al., 2005). Moreover, these interactions are conserved between different plant species (Immink et al., 2002). Despite the fact that many studies have been done in yeast only little information is known about how these interactions occur *in planta*. In this work, different petunia MADS box proteins, the FLORAL BINDING PROTEINS FBP involved in ovule development were used for the study of protein-protein interactions in living cells. First, the genetic fluorescent labels ECFP and EYFP were cloned at the C-terminal side of the different FBPs. C-terminal fusions to various Arabidopsis MADS box proteins appeared to give no loss in biological activity of these proteins Angenent and Urbanus, unpublished. Subsequently, different combinations of the MADS box proteins were transfected in cowpea leaf protoplasts, which transfection has been described previously (Ruscinova et al., 2004).

The localization of the FBP proteins FBP11, FBP2 and FBP24 has been described by Nougalli and colleagues (Nougalli-Tonaco et al., 2006). Differences in sub-cellular localization were observed among the proteins. Remarkably, the single transfected constructs FBP2 and FBP24 were localized in the nucleus, whereas FBP11 stays in the cytoplasm, probably because of its inability to homodimerize, which seems to be a prerequisite for movement into the nucleus (Immink et al., 2002). Co-transfections of FBP2 and FBP24, as well as FBP11 and FBP24, were performed and nuclear co-localization was observed in both cases. Considering that FBP11 is expressed in the cytoplasm by its own, and taking into account the hypothesis that dimerization is essential for transport into the nucleus, the co-localization of both proteins is already a preliminary indication of the formation of dimers. Co-localization is a good indicator for interacting proteins, but, on the other hand, FRET-FLIM measurements can unambiguously prove the existence of physical interactions between the different FBPs.

15.6.2 Molecular interaction imaging via FRET-FLIM

Various techniques to measure FRET have been applied in animal (Bastiaens and Pepperkok, 2000) and in plant cells (Hink et al., 2002; Ruscinova et al., 2004). We have used FLIM by combining a two-photon excitation laser-scanning microscopy with time-correlated single photon counting as described above. First a fluorescence intensity image is obtained. Subsequently, the fluorescence decay of the donor molecule is determined for every pixel in the image. Depending on the fluorescent signal of the donor, an experiment typically takes 90 seconds (Borst et al., 2003). FLIM measurements of the single and double co-transfected cells, as described for the confocal imaging part, were repeated and these experiments started in a specific order. In protoplasts co-expressing the ECFP and EYFP tagged FBPs,

a protoplast was selected showing EYFP fluorescence in the epi-fluorescence mode while ECFP fluorescence is hardly visible in this configuration. If ECFP expression was observed in the 2-photon-imaging mode, this cell was chosen for a FLIM measurement. The excitation wavelength in plant cells was set to 860 nm, which mainly excites the ECFP molecules, whereas excitation of EYFP is minimal. The excitation of ECFP was also reported at 820 nm (Chen et al., 2003) in a ECFP-EYFP pair, but at this wavelength the auto-fluorescence detected with the ECFP band pass filter 480DF30 nm in plant protoplasts is higher than at 860 nm.

In Fig. 15.3A, a monochromatic image represents the fluorescence intensity of the ECFP donor molecules in the absence of EYFP acceptor molecules. This is the control experiment to obtain the fluorescence lifetime of the FBP24-ECFP donor alone. The pixel where the blue crosshair is pointed is the actual fluorescence decay shown in Fig. 15.3B. The fluorescence lifetime image is calculated per pixel and displayed as a pseudo color image. In Fig. 15.3C the fluorescence lifetime of FBP24-ECFP of 2.5 ns clearly shows up throughout the whole nucleus indicated as a blue color. The distribution of fluorescence lifetimes can be observed in Fig. 15.3D. The fluorescence lifetime was analyzed according to a mono-exponential decay fit model. For transcription factors in plant cells a fluorescence lifetime of typically 2.5 ns is found. After determination of the fluorescence lifetime of the donor FBP-ECFP alone, the analysis for all other combinations was performed according to a double exponential decay model, in which the value of the ECFP fluorescence lifetime was fixed to 2.5 ns. Upon FRET the fluorescence lifetime of the ECFP donor molecules will decrease and the amount of reduction is directly correlated with the FRET efficiency. The fluorescence lifetime images displayed in the figures represent the average lifetime values.

In Fig. 15.4 A-B the fluorescence intensity and lifetime images are presented for the co-transfection of FBP2-ECFP and FBP24-EYFP. The fluorescence intensity image clearly shows a nuclear localization. The fluorescence lifetime image indicates a significant reduction of the fluorescence lifetime (τ) dark orange to green corresponds to $\tau = 1.9 - 2.0$ ns. The distribution of fluorescence lifetimes is given in the histogram in Fig. 15.4C. This distribution of fluorescence lifetimes in the case of the combination FBP2-ECFP and FBP24-EYFP was homogeneously spread around 2.0 ns resulting in a FRET efficiency of 20%. The localization of the co-transfection of FBP24-ECFP and FBP11-EYFP is also nuclear, but the distribution of fluorescence lifetimes in this combination is broader than that of the previous pair of proteins. The combination FBP24-ECFP and FBP11-EYFP suggests that there are sub-nuclear regions with $\tau=1.9$ ns and without interaction $\tau=2.4$ ns between the two FBP proteins. This effect is illustrated in Fig. 15.4E where green spots interaction are present in a 'blue' nucleus no interaction. In the histogram Fig. 15.4F a peak at 2.5 ns is seen that is absent in the histogram of Fig. 15.4C. The reciprocal combinations have been tested as well and gave the same results data not shown.

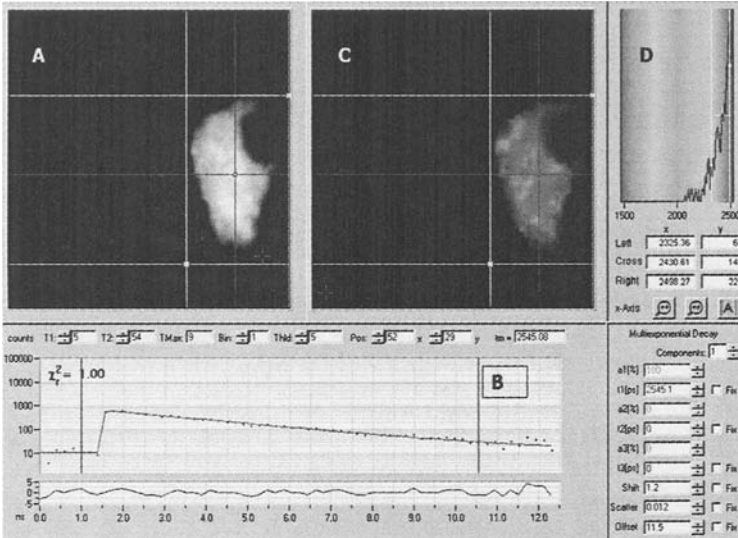


Figure 15.3. An image of a typical FLIM experiment using the Becker and Hickl analysis software. In panel A the fluorescence intensity of the nuclear localized MADS box protein, FBP24-ECFP, is shown. At the blue crosshair the fluorescence decay of the selected pixel is displayed (panel B). The fluorescence lifetimes are calculated per pixel and visualized as a pseudo color image (panels C and D). (See color insert section.)

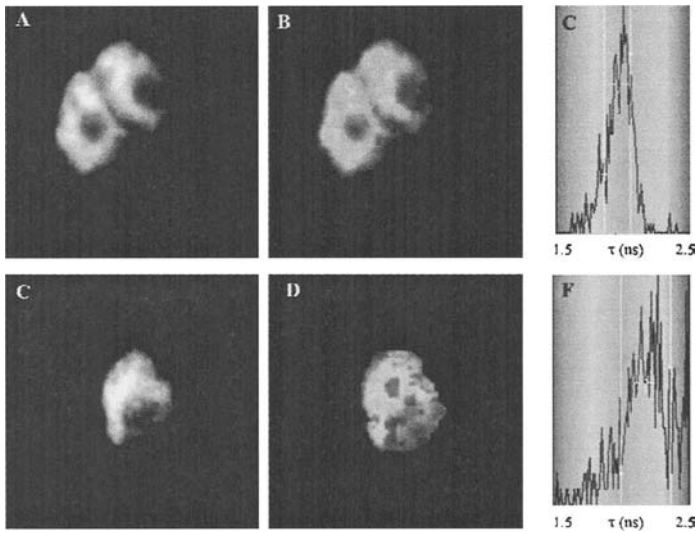


Figure 15.4. FRET-FLIM analyses in double exponential decay model of transfected cowpea leaf protoplasts, expressing the following combinations FBP2-ECFP and FBP24-EYFP (panels A-C) and FBP24-ECFP and FBP11-EYFP (panels D-F). In panels A and D the fluorescence intensity image of the nucleus of a representative cell is shown, in panels B and E the fluorescence lifetime image of the same nucleus is shown as a pseudo color image, and in panels C and F the distribution of fluorescence lifetimes over the nucleus is presented. (See color insert section.)

Several studies revealed that homo- and/or heterodimerization of transcription factors have indicated their binding to specific DNA sequences (Pellegrini et al., 1995; Shore and Sharrocks, 1995). Also higher-order complex formation of MADS box transcription factors is stabilized by specific DNA binding (Egea-Cortines et al., 1999). It might be possible that the sub-nuclear regions represent places where the chromatin is available for transcription and to which the transcription factors are recruited, resulting in stabilization of the less stable or “transient” interactions (Nougalli-Tonaco et al., 2006). The FRET-FLIM data also have shown to be concentration independent. The fluorescence intensity signal over the nucleus is homogeneously distributed, but the fluorescence lifetimes showed sub-nuclear spots with reduced values indicating specific molecular interactions.

It was shown previously by yeast two-hybrid and FRET-FLIM that the petunia flowering gene PFG and FBP2 do not interact (Immink et al., 2002). This combination was used as negative control and the invariant fluorescence lifetimes for different locations in the nucleus indicated no interaction results not shown. As a positive control the combination FBP2-ECFP and FBP11-EYFP was transfected in cells and throughout the whole nucleus average fluorescence lifetimes of about 1.9 ns were measured data not shown (Immink et al., 2002).

15.6.3 Molecular interaction imaging via FRET-FLIM

FRET applications in combination with cell biology have become a very powerful tool to obtain spatial and dynamic information of cellular processes *in vivo*. FRET can be used as a spectroscopic ruler to detect molecular interactions between proteins or molecules in living cells. In this review we have discussed different methodologies to measure FRET and FLIM having several advantages compared to intensity based methods. A good example of the additional valuable information is shown in the highly spatial resolved fluorescence lifetime images Fig. 15.4. FLIM measurements of the MADS box transcription factors showed sub-nuclear spots in the fluorescence lifetime images indicating molecular interactions between the different FBP's. The reduced fluorescence lifetimes in these regions may indicate possible transcriptional activation in the nucleus and these data could not be retrieved with other FRET techniques. Acceptor photobleaching (APB) is a good alternative method to measure FRET, but preferably in combination with FRET biosensors where the molar ratio of ECFP and EYFP is the same and concentration effects are minimal.

How can we improve FLIM measurements in the future? One option is to combine APB with FLIM. The fluorescence lifetime will be determined before and after a bleach pulse and the donor fluorescence lifetime should return to its original value after the destruction of the acceptor (Bastiaens and Squire, 1999). For this method the FLIM set up should be equipped with specific lasers to photobleach the acceptor and the cells need to be fixed to avoid redistribution of the acceptor. An alternative method is the simultaneous

determination of donor and acceptor fluorescence lifetimes. Upon physical interaction between a donor and acceptor molecules the donor fluorescence lifetime will become shorter and the acceptor fluorescence will grow in at the same rate as the donor fluorescence decay rate. In this configuration donor quenching and acceptor fluorescence in-growth is a direct internal prove for the existence of molecular inter-actions and donor quenching is not due to autofluorescent components from the cells.

15.7. ACKNOWLEDGMENTS

We thank Gerco Angenent and Sacco de Vries for continuing interest and fruitful collaboration.

15.8. REFERENCES

- Bastiaens, P. I. and Pepperkok, R., 2000, Observing proteins in their natural habitat: the living cell. *Trends Biochem Sci* **25**, 631-637.
- Bastiaens, P. I. and Squire, A., 1999, Fluorescence lifetime imaging microscopy: spatial resolution of biochemical processes in the cell. *Trends Cell Biol* **9**, 48-52.
- Becker, W., Bergmann, A., Hink, M. A., Konig, K., Benndorf, K. and Biskup, C., 2004. Fluorescence lifetime imaging by time-correlated single-photon counting. *Microscopy Research and Technique* **63**, 58-66.
- Berney, C. and Danuser, G., 2003, FRET or no FRET: A quantitative comparison. *Biophys J* **84**, 3992-4010.
- Borst, J. W., Hink, M. A., van Hoek, A. and Visser, A. J., 2005, Effects of refractive index and viscosity on fluorescence and anisotropy decays of enhanced cyan and yellow fluorescent proteins. *J Fluoresc* **15**, 153-160.
- Borst, J. W., Hink, M. A., van Hoek, A. and Visser, A. J., 2003, Multiphoton microspectroscopy in living plant cells. In *Proceedings of SPIE*, vol. 4963 ed. A. Periasamy and P. T. C. So, pp. 231-238.
- Bunt, G. and Wouters, F. S., 2004, Visualization of molecular activities inside living cells with fluorescent labels. *Int Rev Cytol* **237**, 205-277.
- Burch, L. R., Scott, M., Pohler, E., Meek, D. and Hupp, T., 2004, Phage-peptide display identifies the interferon-responsive, death-activated protein kinase family as a novel modifier of MDM2 and p21 WAF1. *J Mol Biol* **337**, 115-128.
- Campbell, R. E., Tour, O., Palmer, A. E., Steinbach, P. A., Baird, G. S., Zacharias, D. A. and Tsien, R. Y., 2002, A monomeric red fluorescent protein. *Proc Natl Acad Sci USA* **99**, 7877-7882.
- Causier, B. and Davies, B., 2002, Analysing protein-protein interactions with the yeast two-hybrid system. *Plant Mol Biol* **50**, 855-870.
- Chen, Y., Mills, J. D. and Periasamy, A., 2003, Protein localization in living cells and tissues using FRET and FLIM. *Differentiation* **71**, 528-541.
- Clegg, R. M., 1996, in *Fluorescence Imaging Spectroscopy and Microscopy* X. Wang and B. Herman Eds. New York: Wiley.
- De Folter, S., Immink, R. G., Kieffer, M., Parenicova, L., Henz, S. R., Weigel, D., Busscher, M., Kooiker, M., Colombo, L., Kater, M. M., Davies, B. and Angenent, G.C., 2005, Comprehensive interaction map of the arabidopsis MADS Box transcription factors. *Plant Cell* **17**, 1424-1433.
- Egea-Cortines, M., Saedler, H. and Sommer, H., 1999, Ternary complex formation between the MADS-box proteins SQUAMOSA, DEFICIENS and GLOBOSA is involved in the control of floral architecture in *Antirrhinum majus*. *EMBO J* **18**, 5370-9.
- Ferrario, S., Busscher, J., Franken, J., Gerats, T., Vandenbussche, M., Angenent, G. C. and Immink, R. G., 2004, Ectopic expression of the petunia MADS box gene UNSHAVEN accelerates

- flowering and confers leaf-like characteristics to floral organs in a dominant-negative manner. *Plant Cell* **16**, 1490-1505.
- Gadella, T. W., Jr., van der Krogt, G. N. and Bisseling, T., 1999, GFP-based FRET microscopy in living plant cells. *Trends Plant Sci* **4**, 287-291.
- Gerritsen, H. C., Asselbergs, M. A., Agronskaia, A. V. and Van Sark, W. G., 2002, Fluorescence lifetime imaging in scanning microscopes: acquisition speed, photon economy and lifetime resolution. *J Microsc* **206**, 218-224.
- Gerritsen, H. C. and De Grauw, C. J., 1999, Imaging of optically thick specimen using two-photon excitation microscopy. *Microscopy Research and Technique* **47**, 206-209.
- Gordon, G. W., Berry, G., Liang, X. H., Levine, B. and Herman, B., 1998, Quantitative fluorescence resonance energy transfer measurements using fluorescence microscopy. *Biophys J* **74**, 2702-2713.
- Gratton, E., Breusegem, S., Sutin, J. and Ruan, Q. Q., 2003, Fluorescence lifetime imaging for the two-photon microscope: time-domain and frequency-domain methods. *J Biomed Opt* **8**, 381-390.
- Hara, M., Bindokas, V., Lopez, J. P., Kaihara, K., Landa, L. R., Jr., Harbeck, M. and Roe, M. W., 2004, Imaging endoplasmic reticulum calcium with a fluorescent biosensor in transgenic mice. *Am J Physiol Cell Physiol* **287**, C932-938.
- Haupts, U., Maiti, S., Schwille, P. and Webb, W. W., 1998, Dynamics of fluorescence fluctuations in green fluorescent protein observed by fluorescence correlation spectroscopy. *Proc Natl Acad Sci USA* **95**, 13573-13578.
- Herman, B., 1998, Fluorescence Microscopy. BIOS Scientific Publishers, New York.
- Hink, M. A., Bisseling, T. and Visser, A. J. 2002, Imaging protein-protein interactions in living cells. *Plant Mol Biol* **50**, 871-883.
- Ho, F. M. and Hall, E. A., 2004, A strand exchange FRET assay for DNA. *Biosens Bioelectron* **20**, 1001-1010.
- Honma, T. and Goto, K., 2001, Complexes of MADS-box proteins are sufficient to convert leaves into floral organs. *Nature* **409**, 525-529.
- Immink, R. G., Ferrario, S., Busscher-Lange, J., Kooiker, M., Busscher, M. and Angenent, G. C., 2003, Analysis of the petunia MADS-box transcription factor family. *Mol Genet Genomics* **268**, 598-606.
- Immink, R. G. H., Gadella, T. W. J., Ferrario, S., Busscher, M. and Angenent, G. C., 2002, Analysis of MADS box protein-protein interactions in living plant cells. *Proc Natl Acad Sci USA* **99**, 2416-2421.
- Jares-Erijman, E. A. and Jovin, T. M. 2003. FRET imaging. *Nat Biotechnol* **21**, 1387-1395.
- Karpova, T. S., Baumann, C. T., He, L., Wu, X., Grammer, A., Lipsky, P., Hager, G. L. and McNally, J. G., 2003, Fluorescence resonance energy transfer from cyan to yellow fluorescent protein detected by acceptor photobleaching using confocal microscopy and a single laser. *J Microsc* **209**, 56-70.
- Kenworthy, A. K., 2001, Imaging protein-protein interactions using fluorescence resonance energy transfer microscopy. *Methods* **24**, 289-296.
- Kneen, M., Farinas, J., Li, Y. and Verkman, A. S. 1998. Green fluorescent protein as a noninvasive intracellular pH indicator. *Biophys J* **74**, 1591-1599.
- Lakowicz, J. R., 1999, Principles of Fluorescence Spectroscopy, 2nd edition. New York: Kluwer Academic/Plenum Publishers.
- Lippincott-Schwartz, J., Snapp, E. and Kenworthy, A., 2001, Studying protein dynamics in living cells. *Nat Rev Mol Cell Biol* **2**, 444-456.
- Mahajan, N. P., Harrison-Shostak, D. C., Michaux, J. and Herman, B., 1999, Novel mutant green fluorescent protein protease substrates reveal the activation of specific caspases during apoptosis. *Chem Biol* **6**, 401-409.
- Matz, M. V., Fradkov, A. F., Labas, Y. A., Savitsky, A. P., Zaraisky, A. G., Markelov, M. L. and Lukyanov, S. A., 1999, Fluorescent proteins from nonbioluminescent Anthozoa species. *Nat Biotechnol* **17**, 969-973.
- Miyawaki, A., Griesbeck, O., Heim, R. and Tsien, R. Y., 1999, Dynamic and quantitative Ca²⁺ measurements using improved cameleons. *Proc Natl Acad Sci USA* **96**, 2135-2140.
- Miyawaki, A., Llopis, J., Heim, R., McCaffery, J. M., Adams, J. A., Ikura, M. and Tsien, R. Y., 1997, Fluorescent indicators for Ca²⁺ based on green fluorescent proteins and calmodulin. *Nature* **388**, 882-887.

- Morgan, M. J. and Thorburn, A., 2001, Measurement of caspase activity in individual cells reveals differences in the kinetics of caspase activation between cells. *Cell Death Differ* **8**, 38-43.
- Nougalli-Tonaco, I. A., Borst, J. W., Vries, S. C., Angenent, G. C. and Immink, R. G., 2006, In vivo imaging of MADS box transcription factor interactions. *Submitted*.
- Offterdinger, M., Georget, V., Girod, A. and Bastiaens, P. I., 2004, Imaging phosphorylation dynamics of the epidermal growth factor receptor. *J Biol Chem* **279**, 36972-36981.
- Pellegrini, L., Tan, S. and Richmond, T. J., 1995, Structure of serum response factor core bound to DNA. *Nature* **376**, 490-498.
- Peter, M., Ameer-Beg, S. M., Hughes, M. K., Keppler, M. D., Prag, S., Marsh, M., Vojnovic, B. and Ng, T., 2005, Multiphoton-FLIM quantification of the EGFP-mRFP1 FRET pair for localization of membrane receptor-kinase interactions. *Biophys J* **88**, 1224-1237.
- Raicu, V., Jansma, D. B., Miller, R. J. and Friesen, J. D., 2005, Protein interaction quantified in vivo by spectrally resolved fluorescence resonance energy transfer. *Biochem J* **385**, 265-277.
- Riechmann, J. L. and Meyerowitz, E. M., 1997, MADS domain proteins in plant development. *Biol Chem* **378**, 1079-1101.
- Rizzo, M. A., Springer, G. H., Granada, B. and Piston, D. W., 2004, An improved cyan fluorescent protein variant useful for FRET. *Nat Biotechnol* **22**, 445-449.
- Russinova, E., Borst, J. W., Kwaaitaal, M., Cano-Delgado, A., Yin, Y., Chory, J. and de Vries, S. C., 2004, Heterodimerization and Endocytosis of Arabidopsis Brassinosteroid Receptors BRI1 and AtSERK3 BAK1. *Plant Cell* **16**, 3216-3229.
- Shaner, N. C., Campbell, R. E., Steinbach, P. A., Giepmans, B. N., Palmer, A. E. and Tsien, R. Y., 2004, Improved monomeric red, orange and yellow fluorescent proteins derived from *Drosophila* sp. red fluorescent protein. *Nat Biotechnol* **22**, 1567-72.
- Shore, P. and Sharrocks, A. D., 1995, The MADS-box family of transcription factors. *Eur J Biochem* **229**, 1-13.
- Squire, A. and Bastiaens, P. I., 1999, Three dimensional image restoration in fluorescence lifetime imaging microscopy. *J Microsc* **193**, 36-49.
- Suhling, K., Siegel, J., Phillips, D., French, P. M., Leveque-Fort, S., Webb, S. E. and Davis, D. M., 2002, Imaging the environment of green fluorescent protein. *Biophys J* **83**, 3589-3595.
- Terry, B. R., Matthews, E. K. and Haseloff, J., 1995, Molecular characterisation of recombinant green fluorescent protein by fluorescence correlation microscopy. *Biochem Biophys Res Com* **217**, 21-27.
- Tsien, R. Y., 1998, The green fluorescent protein. *Annu Rev Biochem* **67**, 67509-67544.
- Verkhusha, V. V. and Lukyanov, K. A. 2004. The molecular properties and applications of Anthozoa fluorescent proteins and chromoproteins. *Nat Biotechnol* **22**, 289-296.
- Voss, T. C., Demarco, I. A. and Day, R. N., 2005, Quantitative imaging of protein interactions in the cell nucleus. *Biotechniques* **38**, 413-424.
- Wallrabe, H., Elangovan, M., Burchard, A., Periasamy, A. and Barroso, M., 2003, Confocal FRET microscopy to measure clustering of ligand-receptor complexes in endocytic membranes. *Biophys J* **85**, 559-571.
- Wilson, G. S. and Gifford, R., 2005, Biosensors for real-time in vivo measurements. *Biosens Bioelectron* **20**, 2388-2403.
- Wouters, F. S. and Bastiaens, P. I., 1999, Fluorescence lifetime imaging of receptor tyrosine kinase activity in cells. *Curr Biol* **9**, 1127-1130.
- Wouters, F. S., Verveer, P. J. and Bastiaens, P. I. H., 2001, Imaging biochemistry inside cells. *Trends Cell Biol* **11**, 203-211.
- Xia, Z. and Liu, Y., 2001, Reliable and global measurement of fluorescence resonance energy transfer using fluorescence microscopes. *Biophys J* **81**, 2395-2402.
- Xu, X., Gerard, A. L., Huang, B. C., Anderson, D. C., Payan, D. G. and Luo, Y., 1998, Detection of programmed cell death using fluorescence energy transfer. *Nucleic Acids Res* **26**, 2034-2035.
- Zacharias, D. A., Violin, J. D., Newton, A. C. and Tsien, R. Y., 2002, Partitioning of lipid-modified monomeric GFPs into membrane microdomains of live cells. *Science* **296**, 913-916.
- Zhang, J., Campbell, R. E., Ting, A. Y. and Tsien, R. Y., 2002, Creating new fluorescent probes for cell biology. *Nat Rev Mol Cell Biol* **3**, 906-918.